Cellular and Molecular Bioengineering, Vol. 13, No. 1, February 2020 (© 2019) pp. 99–112
https://doi.org/10.1007/s12195-019-00597-w

Tissue Targeting and Ultrasound-Targeted Microbubble Destruction Delivery of Plasmid DNA and Transfection *In Vitro*

YUE WANG,[1] XIAOLI LI,[2] LANLAN LIU,[2] BINGRUO LIU,[3] FENG WANG,[4,5] and CHANGSHENG CHEN[2]

[1]Department of Ultrasound, Peking University Shenzhen Hospital, Shenzhen 518035, People's Republic of China; [2]Key Laboratory of Biomedical Materials and Implant Devices, Research Institute of Tsinghua University in Shenzhen, Nanshan Hi-new Technology and Industry Park, Shenzhen 518057, Guangzhou, People's Republic of China; [3]Division of Engineering Science, University of Toronto, Toronto M5S2E8, Canada; [4]Henan Key Laboratory of Medical Tissue Regeneration, School of Basic Medical Sciences, Xinxiang Medical University, 603 Jinsui Road, Xinxiang 453002, Henan, People's Republic of China; and [5]Shenzhen Kangning Hospital & Shenzhen Mental Health Center, Shenzhen 518003, People's Republic of China

(*Received 8 May 2019; accepted 27 August 2019; published online 4 September 2019*)

Associate Editor David Schaffer oversaw the review of this article.

Abstract

Introduction—Ultrasound-targeted microbubble destruction (UTMD) has been shown a promising approach for target-specific gene delivery and treatment of many diseases in the past decade. To improve the therapeutic potential of UTMD, the gene carrier of microbubbles should possess adequate DNA condensation capability and (or) specific cell or tissue selectivity. The tissue-targeted and ultrasound-targeted cationic microbubbles were developed to meet gene therapy.

Methods—A tissue-targeted stearic acid-inserted cationic microbubbles (SCMBs) were prepared for ultrasound-targeted gene delivery. Branched PEI was modified with stearic acid and further mixed with 1,2-distearoyl-sn-glycero-3-phosphocholine (DSPC) and biot-1,2-distearoyl-sn-glycero-3-phosphoethanolamine-*N*-[methoxy (polyethylene glycol)-2000] (ammonium salt) (Biot-DSPE-PEG2000), intercellular adhesion molecule-1 (ICAM-1) antibody and plasmid DNA to prepare cationic microbubbles through ultrasonic hydration. The ICAM-1 antibody and plasmid DNA were expected to assemble to the surface of SCMBs *via* biotin-avidin interaction and electrostatic interaction, respectively.

Results—It was found that the SCMBs had higher zeta potential compared with neutral microbubbles (NMBs) and cationic microbubbles (CMBs). In contrast, DNA incorporated SCMBs4 showed negative potential, exhibiting good DNA-binding capacity. Confocal images showed that the HeLa cells were attached around by the SCMBs4 from the view of green fluorescence of fluorescein isothiocyanate-loaded IgG which conjugated to ICAM-1 antibody on their surface. After ultrasound treatment, HeLa cells treated with SCMBs exhibited slightly stronger red fluorescence under confocal laser scanning microscope, indicating a synergistic promotion for transfection efficiency.

Conclusions—This tissue- and ultrasound-targeted cationic microbubble demonstrated here showed a promising strategy for improving gene therapy in the future.

Keywords—Gene therapy, Cationic microbubbles, Ultrasound-targeted microbubble destruction (UTMD), Polyethylenimine (PEI), Tissue targeting.

INTRODUCTION

Gene therapy has been shown to be novel and potential strategies for treating or preventing various diseases, namely, cardiovascular disease, malignant tumors, and other genetic diseases.[7,19,24,38] One of most critical challenges for gene therapy is low efficiency of gene delivery to the target tissue, limiting the potential of this type of therapy.[15,16] Currently, a wide variety of lipid- and polymer-based materials have been investigated as vehicles to condense DNA or RNA into nano- (or micro-) complexes that facilitate cellular gene delivery.[1,35] Approaches for improving target selectivity and efficiency of gene expression include development of gene carriers that are selective to specific cell or tissue and (or) responsive to external localized physical triggers.[3,6,17,39] And one robust methodology is based on ultrasound and microbubbles.[17]

Microbubbles are fluorinated gas-filled microparticles made of lipids, saccharide, albumin, biocompatible polymers and other materials.[13,18,28] which collapse under ultrasound through sonoporation, cavitation and other effects.[31]

Address correspondence to Feng Wang, Henan Key Laboratory of Medical Tissue Regeneration, School of Basic Medical Sciences, Xinxiang Medical University, 603 Jinsui Road, Xinxiang 453002, Henan, People's Republic of China; Changsheng Chen, Key Laboratory of Biomedical Materials and Implant Devices, Research Institute of Tsinghua University in Shenzhen, Nanshan Hi-new Technology and Industry Park, Shenzhen 518057, Guangzhou, People's Republic of China. Electronic mails: wfeng100@126.com and ccshbxn@163.com

Ultrasound-targeted microbubble destruction (UTMD) has been widely studied for gene therapy because of its low toxicity, low immunogenicity of vectors, minimum invasiveness, repeatability and effectiveness.[10,27,33] The ultrasound effects can also increase local permeability of tissue and cell membranes to DNA or RNA nano- (or micro-) complexes and augment gene transfer at target sites.[5,11,23] UTMD is definitely a promising strategy to improve efficiency of gene delivery for multiple application, and organs which can be targeted with its high specificity proven by increasing evidences.[8,25,27]

To improve the therapeutic potential of UTMD, the gene carrier of microbubbles should possess adequate DNA condensation capability and (or) specific cell or tissue selectivity. One method is to greatly condense DNA to the microbubbles by incorporating cationic lipids in the microbubbles. As the gold standard of polycations, polyethylenimine (PEI) has been widely used for gene delivery because of its efficient gene expression and the effect of proton sponge.[21,22,30] Another method is to specifically target microbubbles to the cell or tissue of interest by conjugating receptor ligands or antibodies to their surface.[36] As a cell surface glycoprotein, intercellular adhesion molecule-1 (ICAM-1), which is expressed by inflammatory endothelial cells, participates in leukocyte and endothelial adhesion and transmigration.[21] Overexpression of ICAM-1 is considered to be a marker of endothelial cell dysfunction or injury and has been observed in a number of related diseases.[20,34]

Therefore, in the current study, PEI was modified with stearic acid and mixed with 1,2-distearoyl-sn-glycero-3-phosphocholine (DSPC) and biotinylated-1,2-distearoyl-sn-glycero-3-pho-sphoethanolamine-*N*-[methoxy (polyethylene glycol)-2000] (ammonium salt) (Biot-DSPE-PEG2000) to prepare cationic microbubbles (SCMBs), expecting to obtain adequate DNA loading capacity. Intercellular adhesion molecule-1 (ICAM-1) antibody was selected to conjugate to the surface of SCMBs *via* biotin-avidin interaction, aiming to facilitate attachment to the injured paraurethral anterior vaginal wall. The relevant properties of the SCMBs, including concentration, size distribution, zeta potential, and DNA loading capacity were explored. Cytotoxicity, DNA loading capacity and transfection efficiency of the neutral biotinylated NMBs, biotinylated CMBs and SCMBs were studied to evaluate the gene therapy potential of the microbubbles.

MATERIALS AND METHODS

Materials

1,2-Distearoyl-sn-glycero-3-phosphocholine (DSPC) and biot-1,2-distearoyl-sn- glycero-3-phosphoethanolamine-*N*-[methoxy (polyethylene glycol)-2000] (ammonium salt) (Biot-DSPE-PEG2000) were supplied by A.V.T (Shanghai, China). Branched PEI (molecular weight = 600 Dalton, PEI600), stearic acid, chloroform, diethylether, and *N*,*N*′-carbonyl diimidazole (CDI) were purchased from Aladdin (Shanghai, China). Rabbit anti-ICAM1 biotin-conjugated antibody and goat anti-rat IgG/fluorescein isothiocyanate (FITC) antibody were provided by Bioss (Beijing, China). Rat TIMP-1 plasmid containing the red fluorescent protein (RFP) gene was purchased from Vigene Biosciences (Shangdong, China). 3,8-Diamino-5-[3-(diethylmethylammonio)propyl]-6-phenylphenanthridinium diiodide (PI) and Cell Counting Kit-8 were supplied by Beyotime (Shanghai, China).

Preparation and Characterization of Stearic Acid Modified Polyethylenimine 600 (SPEI600)

Stearic acid modified polyethylenimine 600 (SPEI600) was prepared referring to previous literature.[14] Briefly, 0.35 g CDI and 0.6 g stearic acid were dissolved in 10 mL dry chloroform, respectively. Then CDI solution was added drop wise into the stearic acid solution, and stirred with argon protection at room temperature for 2 h. Up to 20 mL branched PEI solution (3.5% (w/v)) was added drop wise into the mixture, and stirred with argon protection at room temperature for 24 h. After the reaction, the solution was precipitated with cold ether (400 mL) and then collected using a centrifuge at 4500 rpm for 10 min. The SPEI600 product was obtained after drying in a vacuum oven. The structure of SPEI600 was verified by proton nuclear magnetic resonance spectroscopy (^{1}HNMR, 400 MHz Bruker Avance DPX-300 spectrometer).

Preparation of Neutral Microbubbles (NMBs), Cationic Microbubbles (CMBs) and SCMBs

Microbubbles were prepared as described by Jin *et al.*[36] In a typical procedure, DSPC, Biot-DSPE-PEG2000, SPEI600 or PEI600 were dissolved in chloroform. Next the solvent was removed by nitrogen

flow and a lipid film was formed. The film was then dried for 4 h under high vacuum to remove the residual chloroform. Buffer consisting of Tris (0.1 M), glycerol, and propylene glycol (volume ratio, 8:1:1) was added into a vessel of dry lipid films to prepare a liposome suspension with a concentration of 3 mg/mL.

Subsequently, the solution was sonicated for 30 min under 55–60 °C by using a bath sonicator (40 kHz, 360 W). The aqueous solution was sealed in a 2 mL penicillin bottle (1 mL each). Air was removed using a vacuum pump, and C_3F_8 was charged into the bottle by using a homemade apparatus. The bottle was ultimately subjected to shock by using a vibrator for 45 s and washing it thrice in a centrifugal tube (400×*g*, 3 min). NMBs, CMB, and SCMB shells of 3 MBs were prepared, and the lipid compositions of the MB shells are summarized as Table 1. Microbubbles were measured and the concentration was determined by using Accusizer 780A (Particle Sizing System, Santa Barbara, USA). Confocal laser scanning microscopy of MB samples was performed on TCS SP8 X (Leica, Solms, Germany).

Characterization of Microbubbles

Zeta potential of SCMBs diluted in PBS, deionized (DI) water and a 10 mM NaCl solution to 10^8 MBs/mL was determined using Zetasizer 3000 (Malvern, Worcestershire, U.K.). NMBs, CMBs, and SCMs diluted in H_2O solution were measured. All samples were measured three times.

Evaluation of DNA-Binding Capacity of SCMBs

For this assay, the microbubbles of different concentrations were diluted by DI water. The concentrations were 1×10^7, 5×10^7, 1×10^8, and 2×10^8 MBs/mL respectively. 0.5 μg plasmid DNA and 1 mL SCMBs suspension of varying concentrations were incubated for 15 min and then washed trice with 10 mM NaCl solution in a centrifugal tube (400×*g*, 3 min) at 4 °C to remove free plasmid DNA. The same SCMB solution at a final volume was destroyed in a bath sonicator heated at about 60 °C for several minutes until the suspension became transparent. The DNA loaded MBs were measured using NanoDrop 2000 (Thermo Scientific, MA, USA).

And next, 10, 20, 30, 40 and 60 μL of plasmid DNA (1 μg/μL) were added to 1 mL of SCMB suspension (5×10^8 MBs/mL) and incubated for 15 min, respectively. Then the suspensions were washed thrice with a 10 mM NaCl solution in a centrifugal tube (400×*g*, 3 min) at 4 °C. Then 10 mM NaCl solution was added to DNA-loaded MB complexes to maintain the same volume (0.5 mL in total). The suspensions were destroyed in a bath sonicator and heated at about 60 °C for several minutes until the suspension became transparent. The solutions were measured using NanoDrop 2000 (Thermo Scientific, MA, USA).

Preparation of Tissue-Targeted SCMBs

Biotinylated monoclonal antibodies can conjugate to the surface of the MBs *via* a streptavidin link. 30 μg streptavidin l was added to 1×10^8 SCMB and incubated with repeatedly and gently blown off for 5 min. After centrifuged and removed the unreacted streptavidin, 10 μL Rabbit anti-ICAM1 biotin-conjugated antibody was added to the suspension with sonication for 15 min at room temperature. SCMBs were washed with DI water three times in a centrifuge at 400×*g* for 3 min at 4 °C to remove excess free ICAM-1. The IgG/FITC antibody was used to show that ICAM-1 was incorporated into the shell of the SCMBs. After binding ICAM-1, the suspension was incubated with 10 μg plasmid DNA for 15 min and washed once with a 10 mM NaCl solution. A PI fluorescence solution was then used to determine whether DNA was loaded on the shell of the SCMBs by electrostatic interaction.

Cell Culture

HeLa cells were cultured with Dulbecco's modified Eagle's medium. The medium was supplemented with 10% fetal bovine serum, 100 U/mL penicillin and

TABLE 1. Percent molar ratio of lipid-based components in the designing microbubbles.

Microbubble	DSPC (20 mg/mL)	Biot-DSPE-PEG2000 (18 mg/mL)	SPEI600	PEI600 (40 mg/mL)
NMBs	92.3	7.7	0	0
CMBs	66.1	5.5	0	28.4
SCMBs1	83.9	6.9	9.2	0
SCMBs2	77.3	6.4	16.3	0
SCMBs3	71.1	5.9	23	0
SCMBs4	66.1	5.5	28.4	0
SCMBs5	61.7	5.1	33.2	0

0.1 mg/mL streptomycin. Cells were cultured in a humidified atmosphere with 5% CO_2 at 37 °C.

Cell Viability Assay

HeLa cells were seeded on 96-well plates, with cell concentration of 1×10^5. NMB, CMB, and SCMB suspension was incubated with plasmid DNA for 15 min at room temperature, respectively. When cell confluence reached 70–80%, NMB/DNA, CMB/DNA, and SCMB/DNA solutions were added. The final concentrations of the DNA and MBs were maintained at 0.5 μg and 1×10^7 MBs/mL each well. Cytotoxicity testing was performed with or without ultrasound exposure. After 24 h incubated, cells were added with Cell Counting Kit-8 for 2 h at 37 °C. Absorbance values at 450 nm was recorded on the FC 680 microplate reader (ThermoFisher, MA, USA).

Evaluation of SCMB Targeting Capability

HeLa cells were seeded on six-well plates. After 24 h incubated, 250 μL SCMBs solution (1×10^7 MBs/mL) was added to each well, the ICAM-1 antibody has been loaded on the shell of SCMBs, and then incubated for 15 min. A medium (250 μL) was then added into the well. The IgG/FITC antibody was used to measure the target of ICAM-1 antibody conjugated SCMBs. Fluorescence microscopy was evaluated on the MF43 fluorescence microscope (Leica, Solms, Germany).

In Vitro Transfection of SCMB-Labeled DNA Carrying MMP9 Gene

10 μg plasmid DNA was added to 250 μL of NMB, CMB, and SCMB solutions (5×10^8 MB/mL), respectively. The solutions were incubated for 15 min under room temperature, followed by washing twice with 10 mM NaCl and centrifugation for 3 min at 2000 rpm to remove the free DNA. HeLa cells were seeded on 6-well plates (1×10^6 cells) and labeled with DNA-carrying SCMBs as earlier described. After incubation for 15 min, wells exposed to ultrasound incubation for 30 s with a sonoporation device (SoniGene System, Visual Sonics, Toronto, Canada) at 1.0 MHz, 2 W/cm^2, and 50% duty cycle. The treated plates were incubated for 6 h in a humidified atmosphere with 5% CO_2 at 37 °C. Subsequently, the medium was replaced with a complete medium and cultured 48 h. Red fluorescent protein RFP was evaluated using the MF43 fluorescence microscope (Leica, Solms, Germany).

Western Blot Analysis

Transfected HeLa cells were lysed in a buffer (pH 8.0) containing 20 mM Tris. HCl, 137 mM NaCl, 1% NP-40, 10% glycerol, 1 mM Na_3VO_4, 1 mM PMSF, 1% aprotinin, and 20 μg/mL leupeptin. Protein concentrations were determined using the Lowry method. For whole cell lysates, Laemmli sample buffer was added and boiled. Equal amounts of protein were separated by SDS-PAGE. The proteins were blotted to PVDF membranes and probed with antibodies for MMP9. Densitometry was conducted using Scion Image (Scion Corporation, Frederick, MD). The quantities of MMP9 were equalized relative to MMP9. All blots were repeated at least three times.

Statistical Analysis

Experimental data were analyzed using SPSS ver. 16.0. The results were presented as the mean ± SD (standard deviation). Multiple groups were statistically analyzed by one-way ANOVA. When the p value was < 0.05 ($p < 0.05$), the data were considered significantly different.

RESULTS

Synthesis and Characterization of SPEI600

Synthesis scheme of SPEI600 was shown in Fig. 1a. Stearic groups were conjugated to PEI using carbonyldiimidazole-activated acids. ^{1}H NMR analysis confirmed that 13% of the PEI amino groups were acylated (Fig. 1b). The chemical shift δ0.9 ppm is assigned to the proton -CH_3 on stearic acid backbone (marked for *a*); δ2.5–2.93 ppm are assigned to the proton –NCH_2CH_2N– protons of the PEI backbone (marked for *e, f, g, h, i, j, k, l* and *m*); δ1.24 ppm is assigned to the proton $(CH_2)_{14}$ on PEI backbone (marked for *b*); δ1.58 ppm and δ2.13–2.17 ppm are assigned to the proton –$COCH_2CH_2$– on stearic acid (marked for *c* and *d*); and δ2.93–3.3 ppm are assigned to the proton –$CONHCH_2$– on PEI backbone (marked for *n* and *o*).

Preparation and Characterization of MBs

In SPEI, the hydrophobic stearic groups were randomly distributed along the PEI backbone chains to form core–shell structure. This structure had a highly similar conformation like phospholipid shells, which are conducive to form MBs. As shown in Fig. 2, SPEI,

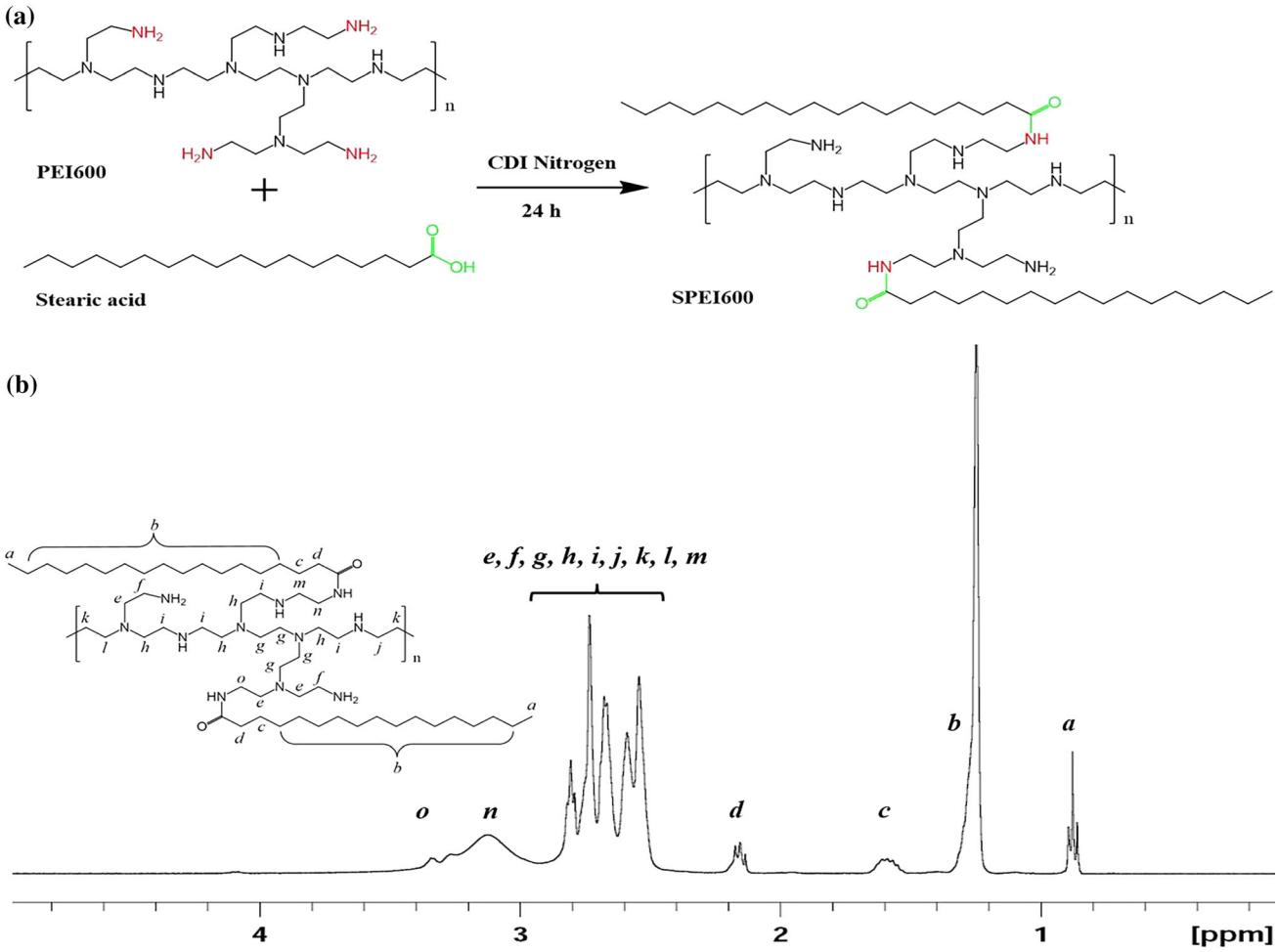

FIGURE 1. Synthesis and characterization of SPEI600. (a) Schematic illustration of synthesis of SPEI600. (b) ^{1}H-NMR spectra of SPEI in $CDCl_3$. The chemical shift δ0.9 ppm is assigned to the proton $-CH_3$ on stearic acid backbone (marked for *a*); δ2.5–2.93 ppm are assigned to the proton $-NCH_2CH_2N-$ protons of the PEI backbone (marked for *e, f, g, h, i, j, k, l* and *m*); δ1.24 ppm is assigned to the proton $(CH_2)_{14}$ on PEI backbone (marked for *b*); δ1.58 ppm and δ2.13–2.17 ppm are assigned to the proton $-COCH_2CH_2-$ on stearic acid (marked for *c* and *d*); and δ2.93–3.3 ppm are assigned to the proton $-CONHCH_2-$ on PEI backbone (marked for *n* and *o*).

DSPC and DSPE-PEG(2000)-Biotin were self-assembled to form SCMB under a C_3F_8 environment. The biotin tag incorporated in the microbubble shell can further combined with ICAM-1-biotin antibodies in the suspension *via* the existence of avidin by biotin-avidin interaction, leading the tissue-targeted SCMBs. The SPEI could enhance the DNA-loading capability of the SCMBs, which were expected to exert ultrasound-mediated DNA transfection. To determine a suitable concentration of SPEI600 in the shell of SCMBs, SCMBs1, SCMBs2, SCMBs3, SCMBs4, and SCMBs5 were prepared with varying amount of the components. Figure 3a showed that with the increase of the SPEI600 mol ratio, the mean diameters of SCMBs increased, ranging from 2.4 to 3.9 μm. However, no significant differences were found for median diameter, ranging from 1.7 to 2.1 μm. Figure 3b showed that the increased amount of SPEI600 enhanced the zeta potential of the SCMBs. The zeta potential values of SCMBs1, SCMBs2, SCMBs3, SCMBs4 and SCMBs5 in DI water were 20.33 $\pm$ 1.44, 40.93 $\pm$ 1.07, 44.63 $\pm$ 1.64, 45.28 $\pm$ 1.76, and 52.73 $\pm$ 0.91 mV, respectively. The zeta potential values of SCMBs increased with the addition amount of SPEI600 and showed significantly higher than CMBs and NMBs, which were $-$ 12.97 $\pm$ 0.75 and 1.93 $\pm$ 0.42 mV, respectively. The cytotoxicity of the different types of SCMBs was assessed using the CCK-8 assay (Fig. 3c). The cell viability of SCMBs4 was $>$ 90%, exhibiting low cytotoxicity. The SCMBs4 was determined to had a defined structure of dark circular rings with bright C_3F_8 gas cores (Fig. 3d).

Three different dispersion medium of SCMBs4 were chosen to evaluate their properties. Figure 4a showed that the zeta potential values of the same concentration of SCMBs4 dispersed in H_2O, 10 mM NaCl, and PBS were 45.28 $\pm$ 1.76, 16.93 $\pm$ 0.63 and 0.96 $\pm$ 0.14 mV, respectively. Especially for SCMBs4, SCMBs4 dis-

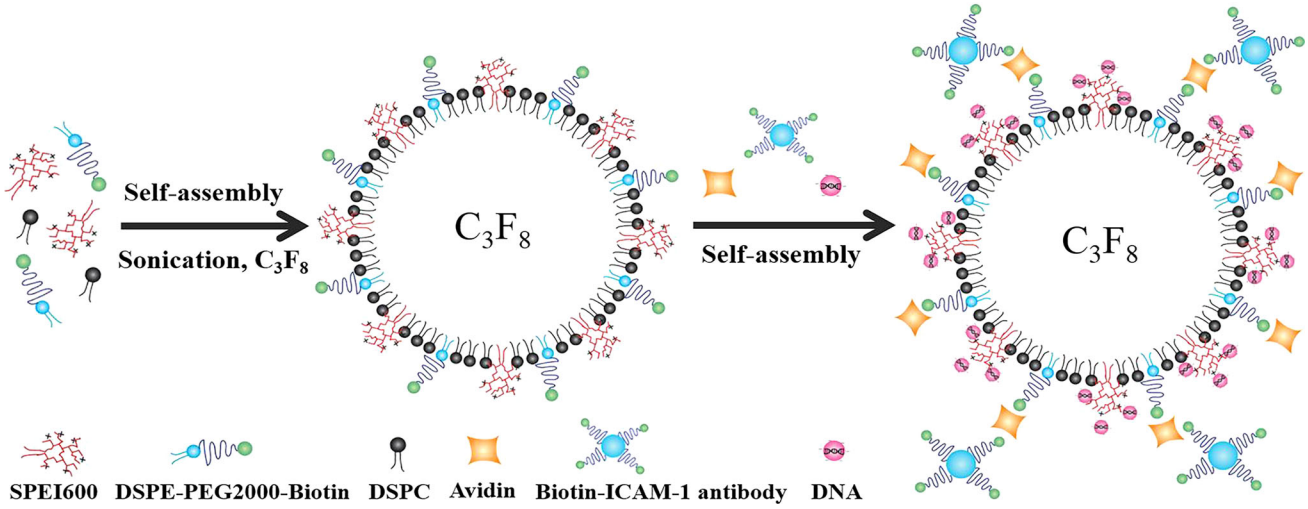

FIGURE 2. Schematic illustration of self-assembly and formation of cationic microbubbles. SPEI600, DSPC and DSPE-PEG(2000)-Biotin first self-assembled to form SCMBs under a C_3F_8 environment. Then biotinylated ICAM-1 assembled onto the shell of the SCMBs by avidin–biotin interaction. Meanwhile the plasmid DNA can further assemble on the SCMBs through electrostatic interaction because of the presence of SPEI600 on the SCMBs, and finally forming the HeLa cell targeted SCMBs/ICAM-1/DNA complex.

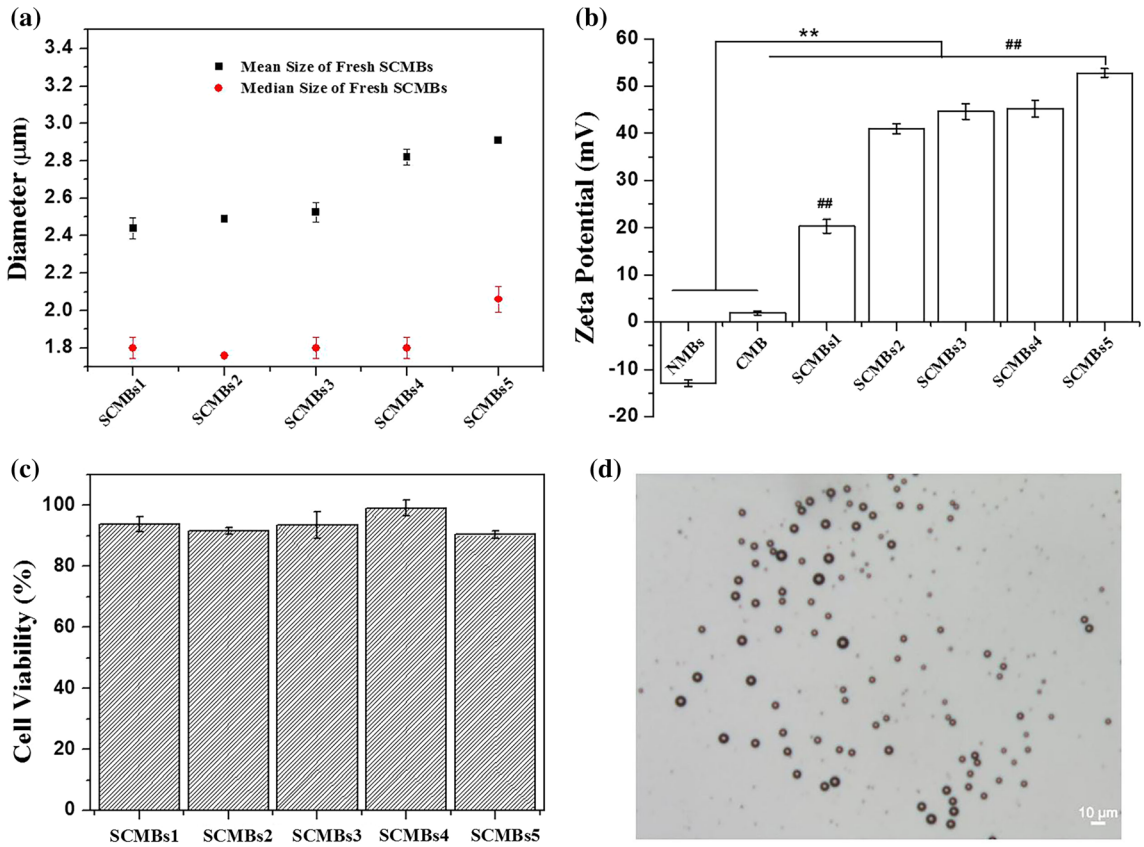

FIGURE 3. Characterization of the microbubbles. (a) Mean and median size of SCMBs with varying ratios of the components. (b) Zeta potential of NMBs, CMBs, and series of SCMBs. $^{**}p < 0.01$ compared with the NMBs and CMB groups, $^{\#}p < 0.01$ compared with the SCMBs 2–4 group, $^{\#\#}p < 0.01$ compared with the SCMBs2-5 group. (c) Cell cytotoxicity assay of the SCMBs. Cell viability was measured using the CCK-8 assay after 24 h. (d) Bright-field images of SCMBs4. All microbubbles were washed with water. Scale bar: 10 μm.

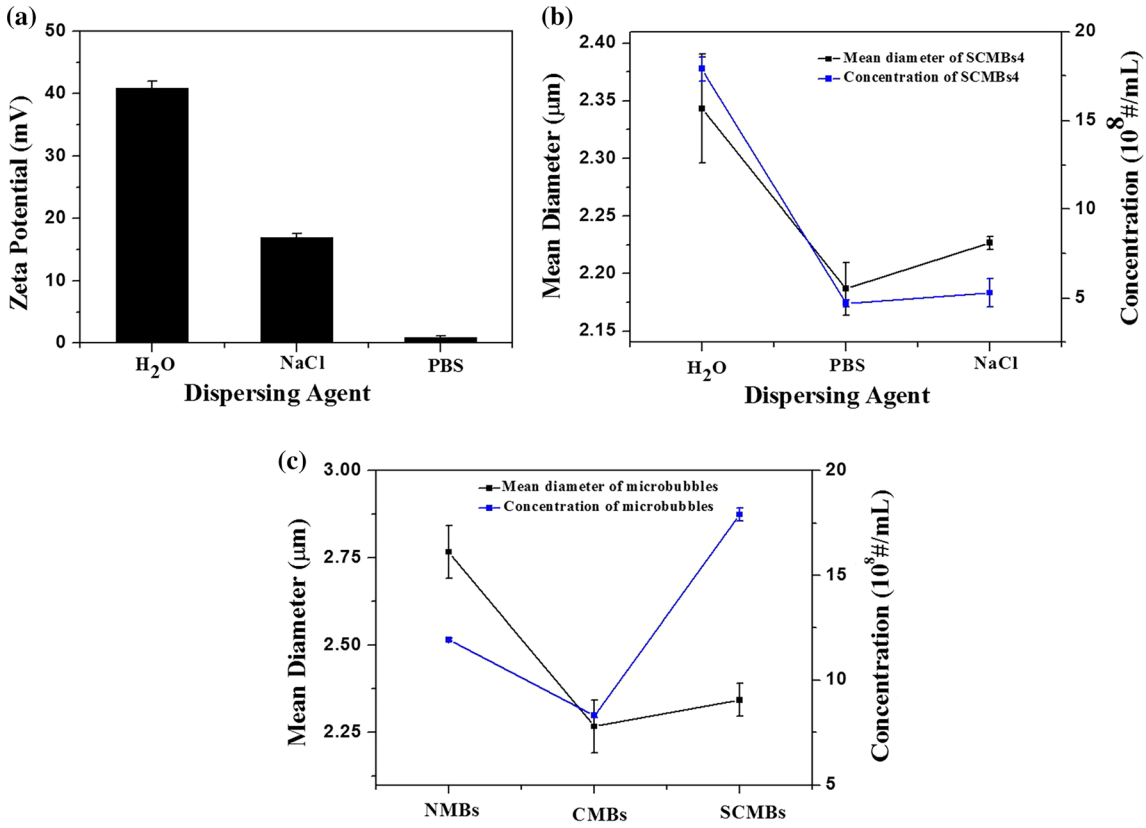

FIGURE 4. Zeta potential, size distribution and concentration of SCMBs4 *via* dealing with DI water, NaCl solution and PBS, respectively. And the size distribution of NMBs, CMBs, and SCMBs4. (a) Zeta potential of SCMBs4 after dealing with DI water, NaCl solution and PBS, respectively. (b) Size distribution and concentration of SCMBs4 after dealing with DI water, NaCl solution and PBS, respectively. (c) Size distribution and concentration of NMBs, CMBs and SCMBs4.

persed in H_2O showed the maximum zeta potential, concentration, and mean diameter (Fig. 4b). The concentration and mean diameter of SCMBs4 were $(17.9 \pm 0.68) \times 10^8$ MBs/mL and 2.34 ± 0.047 μm, respectively. DI water is more suitable for SCMBs4 to maintain positive charge for DNA loading. Figure 4c showed that the concentrations of NMBs, CMBs and SCMBs were $(11.94 \pm 0.08) \times 10^8$ MBs/mL, $(8.31 \pm 0.1) \times 10^8$ MBs/mL, and $(17.9 \pm 0.68) \times 10^8$ MBs/mL. And the mean diameters of NMBs, CMBs, and SCMBs were 2.77 ± 0.08, 2.67 ± 0.07, and 2.34 ± 0.05 μm, respectively.

ICAM-1 Antibody and Plasmid DNA Binding on the SCMBs4

To prepare SCMBs4 for targeted delivery, biotinylated ICAM-1 monoclonal antibodies was conjugated on the shell of biotinylated SCMBs4 *via* a streptavidin link. FITC-labeled secondary antibody IgG was used to combine with ICAM-1 antibody. Figure 5a showed that ICAM-1 antibody was successfully conjugated on the surface of SCMBs4 by the green fluorescence of FITC. After incubation of the plasmid DNA and SCMBs4 for 15 min, DI water was used to wash unbound DNA. The zeta potential of SCMBs4 significantly decreased from 45.28 ± 1.76 mV to -20.21 ± 0.61 mV (Fig. 5b), proving that plasmid DNA was connected on the surface of SCMBs4 successfully by electrostatic interaction. After washing the DNA and SCMBs4 complex with 10 mM NaCl solution, a small amount of DNA was loaded on SCMBs4 (Fig. 5c). And the amount of attached DNA increased as concentration of SCMBs4 increased (Fig. 5c).

To evaluate the DNA-loading capacity of SCMBs4, the same concentration of SCMBs4 (5×10^8 MBs/mL) was incubated, followed by varying amounts of plasmid. Figure 5d showed that DNA-loading capacities were 9.25 ± 0.17, 15.92 ± 0.25, 18.77 ± 0.36, and 23.475 ± 0.31 μg after adding with 10, 20, 30 and 40 μg of plasmid DNA, respectively. It was found there is no difference for DNA loading amount with a step further addition of plasmid DNA to 60 μg. And an amount of 23.5 μg plasmid DNA can be fully loaded on the SCMBs4 at a concentration of 2×10^8 MB/mL. To evaluate the ICAM-1 antibody and plasmid DNA bound on the surface of SCMBs4, FITC-labeled IgG and PI were used for staining. Fig-

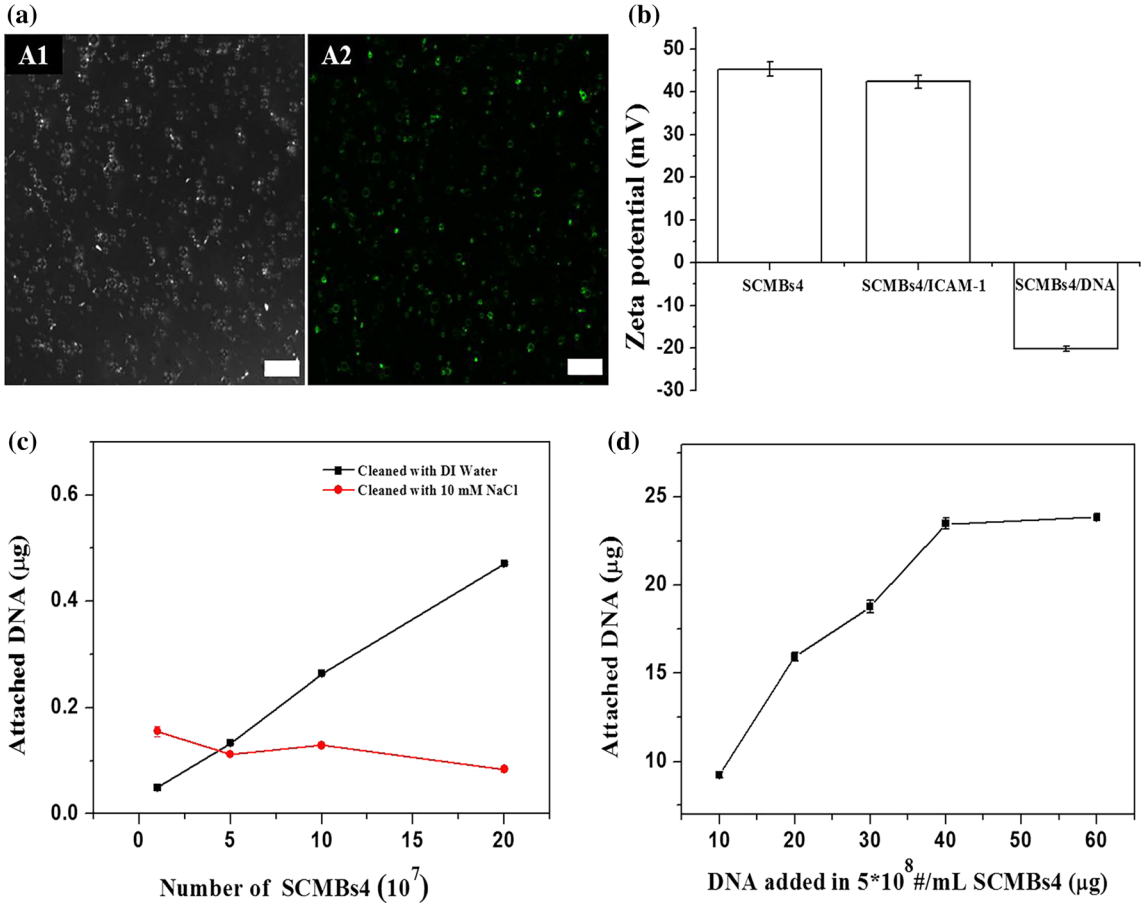

FIGURE 5. The Binding capacity of antibody ICAM-1 and plasmid DNA on SCMBs4. (a) Confocal images of SCMBs4/ICAM-1/DNA complex. (a1) Bright-field microscopy and (a2) green fluorescence microscopy images. Scale bar: 25 μm. (*b*) Zeta potential of SCMBs4, SCMBs4/ICAM-1 complex, and SCMBs4/ICAM-1/DNA complex. The SCMBs4 has a concentration of 10^7 MBs/mL. (c) DNA binding capacity with varying amount of SCMBs4 after cleaning by DI water or 10 mM NaCl solution. The total amount of plasmid DNA is 0.5 μg. (d) The relationship of DNA loading capacity of SCMBs4 at a concentration of 5 $\times$ 10^8/mL with varying amounts of plasmid.

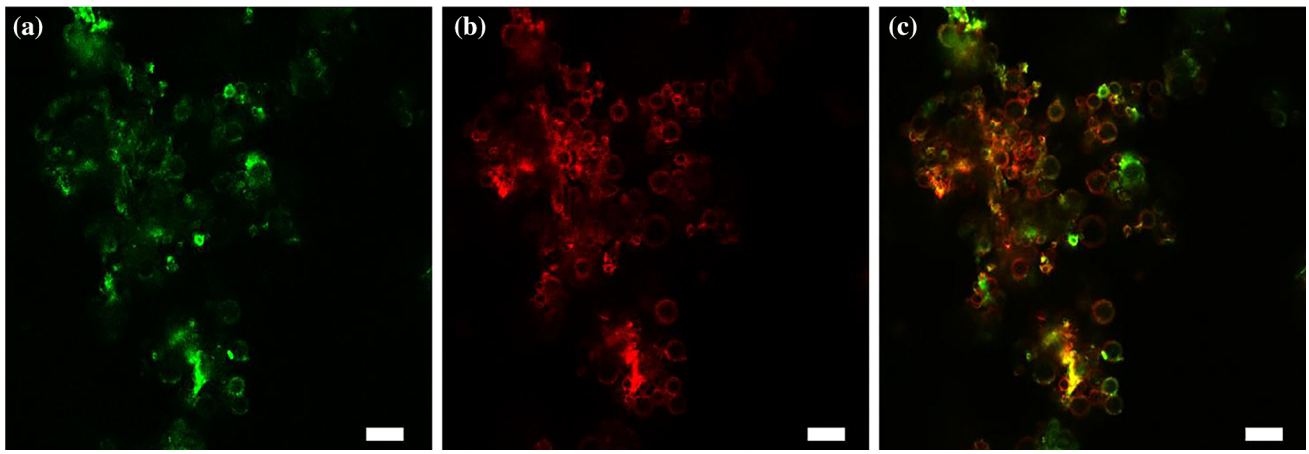

FIGURE 6. Confocal images of SCMBs4/ICAM-1/DNA complex. (a) Green fluorescence excited by 488 nm, indicating binding of ICAM-1 and SCMBs4. (b) Red fluorescence excited by 535 nm, indicating binding of PI-DNA and SCMBs4. (c) Overlaying fluorescence excited by 488 and 535 nm. Scale bar: 10 μm.

ure 6 showed that fluorescent labeled ICAM-1 antibody (green fluorescent) and plasmid DNA (red fluorescent) were clearly marked on the bubble surface.

Cytotoxicity Levels and Targeting Cell Capacity of Microbubbles

To evaluate the cytotoxicity of the microbubbles. NMB/DNA, CMB/DNA and SCMBs4/DNA were incubated with or without ultrasound treatment. HeLa cells were incubated with the MB solution. The cells treated with NMB/DNA, CMB/DNA and SCMBs4/DNA under ultrasound exposure exhibiting cell viabilities of 69.17, 44.71, and 63.4%, respectively. Every group exhibited high cytotoxicity. However, with no ultrasound treatment, CMB/DNA exhibited a slightly lower cell viability than those of NMB/DNA and SCMBs4/DNA (Fig. 7a). Figures 3c and 7a showed no significant differences in cell viability between SCMBs4 and SCMBs4/DNA under normal condition. Ultrasound exposure maybe exert potentially toxic effects on the cells. CMB/DNA exhibited higher cytotoxicity with ultrasound exposure, compared with SCMBs4/DNA ($p < 0.01$). And PEI600 and SPEI600 have the same percent molar ratios in the preparation of CMBs and SCMBs4.

To verify the targeting capacity of MBs, HeLa cells were incubated with ICAM-1 antibody conjugated SCMBs4 with washing by PBS thrice. FITC-labeled IgG was used to stain ICAM-1 antibody on SCMBs4. As shown in Figs. 7b1 and 7b2, HeLa cells are in a dispersed state, with very few of SCMBs4 (with anti-ICAM-1 free) attached around, and there is no fluorescence displayed on the bubble surface under confocal images. However, for the anti-ICAM-1 SCMBs4 group as shown in Figs. 7b3 and 7b4, HeLa cells aggregated to a certain extent with a number of anti-ICAM-1 SCMBs4 attached around, which is further certificated by the strong green fluorescence based on the conjugation of IgG/FITC antibody and anti-ICAM-1 on the bubble surface. Thus, SCMBs can acted on the target cells.

Transfection Efficiency of Plasmid-Loaded Microbubbles

Fluorescence microscopy was employed to further study the intracellular uptake of three types of MBs with or without ultrasound treatment. Figure 8 showed that the cells in NMB samples existed no red fluorescence. However, the cells in the CMBs and SCMBs samples, either with sonication or without sonication, showed strong red fluorescence, and the presence of red fluorescence with sonication is slightly stronger than that without sonication (Figs. 8b, 8c, 8e and 8f). And strongest red fluorescence was observed in SCMBs with sonication (Fig. 8f), indicating ultrasound can synergistically promote gene transfection efficiency.

MMP9 Protein Expression Levels in HeLa Cell

Western blot analysis was conducted to detect the protein expression levels of MMP9 transfected in HeLa cells with three types of MBs without ultrasound exposure (control group, NMBs, CMBs, and SCMBs) and with ultrasound exposure (control + U, NMBs + U, CMBs + U, and SCMBs + U). The protein expression levels of MMP9 in groups with ultrasound exposure significantly increased, relative to those of the corresponding groups without ultrasound exposure ($p < 0.01$) (Fig. 9). And the protein expression level of MMP9 in the SCMBs + U group was the highest and was significantly increased relative to the first six groups ($p < 0.01$) (Fig. 9b).

DISCUSSION

This study reported on the synthesis of a targeted cationic microbubble using SPEI600, DSPC and and Biot-DSPE-PEG2000. We found that DI water as the dispersant agent of MBs exhibited the highest zeta potential, size, and concentration. ICAM-1 antibody and plasmid DNA could be bind to the surface of SCMBs *via* biotin-avidin interaction and electrostatic adsorption. The SCMBs exhibited significantly higher DNA-binding capacity because of its higher zeta potential compared with those of NMBs and CMBs. Additionally, we proved that targeted MBs *via* SCMBs were attached to the HeLa cells by FITC-loaded IgG binding to the ICAM-1 antibody which was conjugated on the surface of the MBs. By UTMD, we found the effective uptake of plasmid DNA by HeLa cells, resulting in significant RFP expression by HeLa cells after ultrasound-guided transfection with plasmid DNA loaded MBs, without compromising the viability of HeLa cells.

Currently, numerous studies have been conducted on the development of a safe and efficient nonviral gene delivery system for gene therapy. MBs have shown potential advantage for application in gene delivery by loading therapeutic molecules into or onto their shells[9,12] UTMD is a potential targeting approach for gene delivery. Sonoporation, which targets the delivery of genes into a specific tissue, had been successfully applied.[2,29] However, ineffective targeted gene delivery had limited the application of this therapy. CMBs could enhanced the capacity of DNA loading efficiency by electrostatic interaction.[32] Currently, one

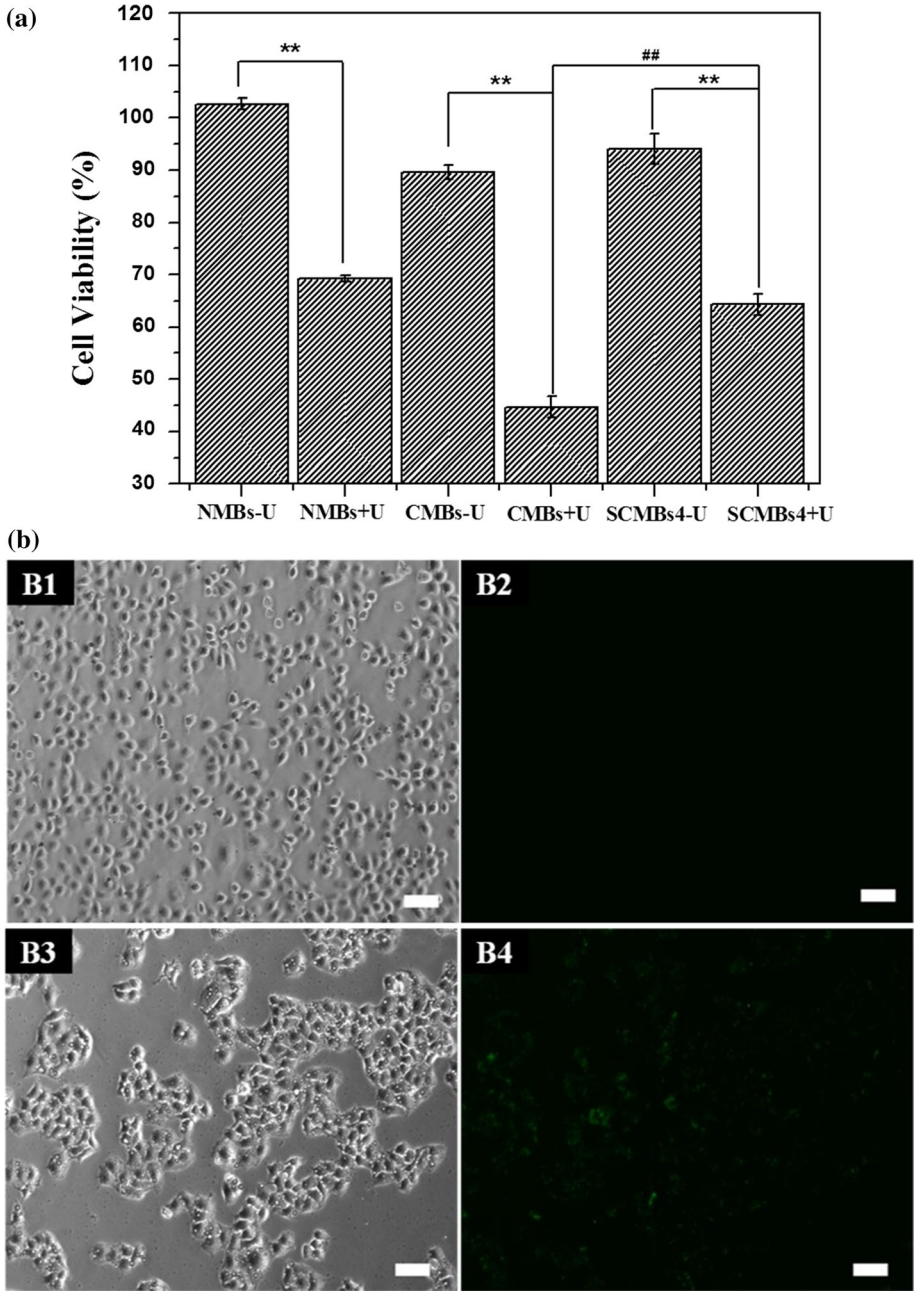

FIGURE 7. Cytotoxicity of HeLa cells treating with various microbubbles and ultrasonic treatment. (a) Cell viability of HeLa cells treating with NMBs, CMBs, and SCMBs4 with or without ultrasonic treatment by CCK-8 assay ($n = 5$). $^{**}p < 0.01$ compared with corresponding group without ultrasonic treatment, $^{\#\#}p < 0.01$ compared with CMBs + U group. (b) Fluorescent images of SCMBs4 targeted to HeLa cells by confocal laser scanning microscopy. (b1) Bright-field microscopy image for SCMBs4 (with anti-ICAM-1 free) treating. (b2) Fluorescent image by exciting at 488 nm for SCMBs4 (with anti-ICAM-1 free) treating. (b3) Bright-field microscopy image for anti-ICAM-1 SCMBs4 treating. (b4) Fluorescent image by exciting at 488 nm for anti-ICAM-1 SCMBs4 treating. Scale bar: 50 μm.

of the strategies for preparing CMBs is combining some cationic lipids (DMTAP, DOTAP, DPTAP, and DSTAP) into the MB shell.[14,29,32] Borden *et al.* prepared a novel application of preformed lipid-coated MBs attached multiple layers of DNA and poly-L-lysine layer-by-layer assembly to increase the DNA loading capacity.[4] The effectiveness of DNA loading was enhanced, but the concentration of DNA was considerably limited. Branched PEI, a cationic polymer, had been widely used to prepare CMBs and showed to be relatively successful as a non-viral gene delivery vector.[26] High-molecular-weight PEI (PEI25000) exhibit high transfection efficiency on the one hand and high cytotoxicity on the other hand.

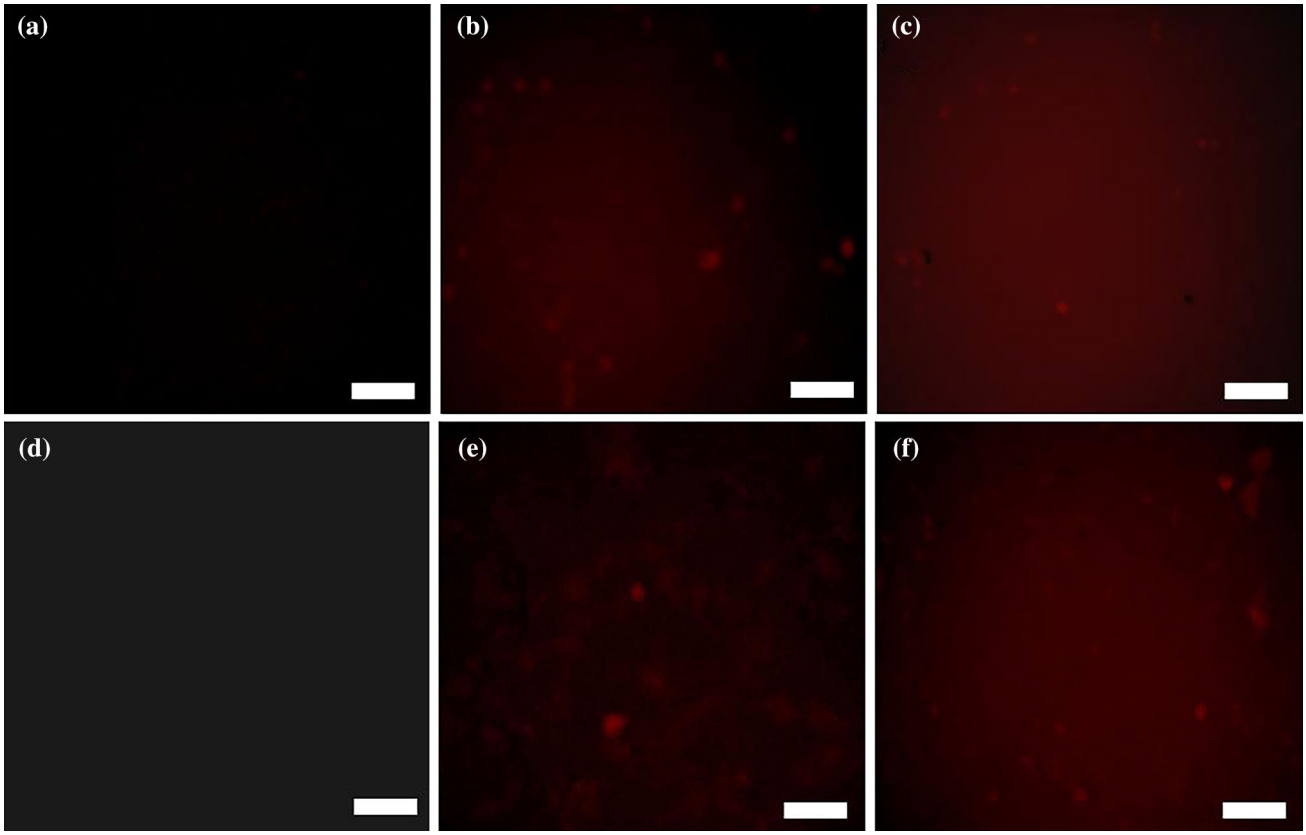

FIGURE 8. Fluorescence photographs of NMBs, CMBs and SCMBs exposed without ultrasound (a–c) and with ultrasound (d–f), respectively. (a, d) NMBs. (b, e) CMBs. (c, f) SCMBs. Scale bar = 100 μm.

Thus, owing to its relatively low cytotoxicity PEI600 had been most widely used for the preparation of CMBs. The zeta potential of the MBs was increased because of PEI600 and DNA loading on the surface of CMBs by electrostatic interaction. By ultrasound destruction, DNA-loaded MBs were delivered to the target tissue by sonoporation.[26,32] Several studies had demonstrated that the concentration of cationic polymers affects the zeta potential, size distribution, and concentration of the MBs[14] which affect the DNA loading efficiency. As the concentration of cationic polymers increased, the transfection efficiency of CMBs also increased.[29] The effectiveness of DNA was increased because of the higher concentration, larger surface area, and higher zeta potential of the MBs.[4,14]

In the current study, stearic acid was modified to PEI600 to generate SPEI600. Each PEI600 molecule was connected to nearly two stearic groups, which were randomly distributed along the PEI backbone chains. The zeta potential of SCMBs was increased with the amount of SPEI600 accumulated. One of the main reasons was the ionic strength of SPEI600. With different cleaning fluids, SCMBs obtained different zeta potential values. Zeta potential was sensitive to the pH and the ionic characteristic of the suspending medium.[14,37] In addition, biotinylated lipid (Biot-DSPE-PEG2000) was incorporated onto its shell, and as expected, biotin-ICAM-1 antibody was linked *via* avidin as bridge. The SCMBs exerted a direct impact on the interactions with target cells or on the ultrasound-mediated gene transfer. In the present study, the DNA loading capacity of SPEI600 was measured to be about 23.475 ± 0.31 μg, which was higher than DSTAP MBs that previously reported. This occurrence might be attributed to steric hindrance. Sun *et al.* synthesized a CMB with DOTMA, aimed to enhancing its DNA-carrying capacity to improve targeted gene transfection; the binding capacity was 20.8 μg.[8] The acid-labile polymer had been shown to exhibit higher gene transfection and lower cytotoxicity. The reason showed that acid-labile polymer degradation reduced the possibility of generating undesirable cytotoxicity.[4] In the present study, the SCMBs showed low cytotoxicity and higher DNA transfection, compared with CMBs. The result of Western blot analysis indicated that transfection efficiency was higher in SCMBs with ultrasound exposure than any other groups.

In conclusion, we developed tissue-targeted CMBs. The tissue-targeted CMBs showed high DNA-binding capacity and HeLa cells targeting capability. With

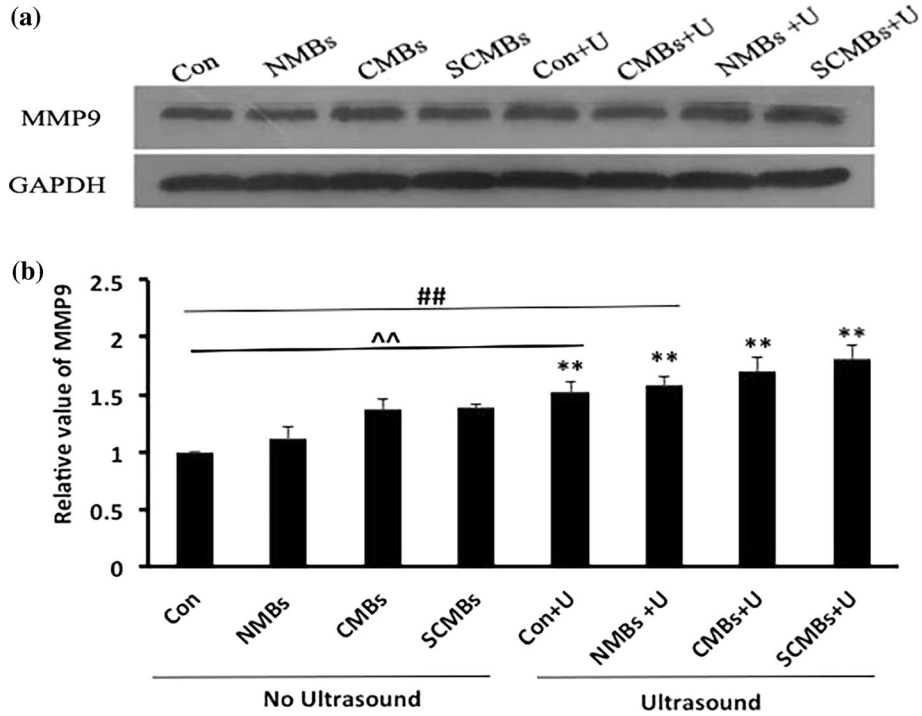

FIGURE 9. MMP9 protein expression levels in HeLa cells. The cell samples were homogenized and processed for Western blot analysis by using an anti-MMP9 antibody. This procedure was conducted using GAPDH as an internal standard. (a) Relative protein expression level of MMP9 in renal macrophages. (b) Protein expression level of MMP9 was quantitatively analyzed. The results were presented as mean ± SD, $^{**}p < 0.01$ compared with the corresponding group without ultrasound exposure, $^{\#\#}p < 0.01$ compared with the first six groups, $^{\wedge\wedge}$compared with the first five groups.

ultrasound treatment, the tissue-targeted CMBs exhibited high transfection efficiency in HeLa cells from a view of strong red fluorescence under confocal laser scanning microscope. While further *in vivo* investigations are required to fully validate the materials, it can be concluded that this tissue-targeted and ultrasound-targeted cationic microbubbles present a promising strategy for improving gene therapy in the future.

ACKNOWLEDGMENTS

Yue Wang, Xiaoli Li, Lanlan Liu, Bingruo Liu, Feng Wang and Changsheng Chen declare that they have no conflict of interest. This work was supported by the National Natural Science Fund of China-Henan Joint Fund (Grant No. U1804187), the Natural Science Foundation of Guangdong Province (Grant No. 2015A030401013) and Shenzhen Science and Technology Projects (Grant Nos. JCYJ20150403091443301, GJHS20170314153414860, JCYJ20170413100222613).

ETHICAL APPROVAL

No human studies were carried out by the authors for this article. All animal studies were carried out in accordance with the Institutes of Health Guide for the Care and Use of Laboratory Animals and approved by the Animal Use Committee of Peking University Shenzhen Hospital (ID# Number: 20170615).

REFERENCES

[1]Al-Dosari, M. S., and X. Gao. Nonviral gene delivery: principle, limitations, and recent progress. *AAPS. J.* 11(4):671–681, 2009.
[2]Anderson, C. D., S. Moisyadi, A. Avelar, C. B. Walton, and R. V. Shohet. Ultrasound-targeted hepatic delivery of factor IX in hemophiliac mice. *Gene Ther*. 23(6):509–510, 2016.
[3]Bae, Y., S. J. Song, J. Y. Mun, K. S. Ko, J. Han, and J. S. Choi. Apoptin gene delivery by the functionalized polyamidoamine (PAMAM) dendrimer modified with ornithine induces cell death of HepG2 Cells. *Polymers (Basel)* 9(6):E197, 2017.
[4]Borden, M. A., C. F. Caskey, E. Little, R. J. Gillies, and K. W. Ferrara. DNA and polylysine adsorption and multi-

layer construction onto cationic lipid-coated microbubbles. *Langmuir* 23(18):9401–9408, 2007.
[5]Burke, C. W., J. S. Suk, A. J. Kim, Y. H. Hsiang, A. L. Klibanov, J. Hanes, and R. J. Price. Markedly enhanced skeletal muscle transfection achieved by the ultrasound-targeted delivery of non-viral gene nanocarriers with microbubbles. *J. Control Release*. 162(2):414–421, 2012.
[6]Chertok, B., R. Langer, and D. G. Anderson. Spatial control of gene expression by nanocarriers using heparin masking and ultrasound-targeted microbubble destruction. *ACS Nano*. 10(8):7267–7278, 2016.
[7]Daigeler, A., A. M. Chromik, K. Haendschke, S. Emmelmann, M. Siepmann, K. Hensel, G. Schmitz, L. Klein-Hitpass, H. U. Steinau, M. Lehnhardt, and J. Hauser. Synergistic effects of sonoporation and taurolidin/TRAIL on apoptosis in human fibrosarcoma. *Ultrasound Med. Biol*. 36(11):1893–1906, 2010.
[8]Danialou, G., A. S. Comtois, R. W. Dudley, J. Nalbantoglu, R. Gilbert, G. Karpati, D. H. Jones, and B. J. Petrof. Ultrasound increases plasmid-mediated gene transfer to dystrophic muscles without collateral damage. *Mol. Ther*. 6(5):687–693, 2002.
[9]De Temmerman, M. L., H. Dewitte, R. E. Vandenbroucke, B. Lucas, C. Libert, J. Demeester, S. C. De Smedt, I. Lentacker, and J. Rejman. mRNA-Lipoplex loaded microbubble contrast agents for ultrasound-assisted transfection of dendritic cells. *Biomaterials* 32(34):9128–9135, 2011.
[10]Deng, Q., B. Hu, S. Cao, H. N. Song, J. L. Chen, and Q. Zhou. Improving the efficacy of therapeutic angiogenesis by UTMD-mediated Ang-1 gene delivery to the infarcted myocardium. *Int. J. Mol. Med*. 36(2):335–344, 2015.
[11]Deng, C. X., F. Sieling, H. Pan, and J. Cui. Ultrasound-induced cell membrane porosity. *Ultrasound Med. Biol*. 30(4):519–526, 2004.
[12]Endo-Takahashi, Y., Y. Negishi, A. Nakamura, D. Suzuki, S. Ukai, K. Sugimoto, F. Moriyasu, N. Takagi, R. Suzuki, K. Maruyama, and Y. Aramaki. pDNA-loaded Bubble liposomes as potential ultrasound imaging and gene delivery agents. *Biomaterials* 34(11):2807–2813, 2013.
[13]Fujii, H., Z. Sun, S. H. Li, J. Wu, S. Fazel, R. D. Weisel, H. Rakowski, J. Lindner, and R. K. Li. Ultrasound-targeted gene delivery induces angiogenesis after a myocardial infarction in mice. *JACC Cardiovasc. Imaging*. 2(7):869–879, 2009.
[14]Jin, Q., Z. Wang, F. Yan, Z. Deng, F. Ni, J. Wu, R. Shandas, X. Liu, and H. Zheng. A novel cationic microbubble coated with stearic acid-modified polyethylenimine to enhance DNA loading and gene delivery by ultrasound. *PLoS ONE* 8(9):e76544, 2013.
[15]Katz, M. G., A. S. Fargnoli, L. A. Pritchette, and C. R. Bridges. Gene delivery technologies for cardiac applications. *Gene Ther*. 19(6):659–669, 2012.
[16]Katz, M. G., A. S. Fargnoli, R. D. Williams, and C. R. Bridges. The road ahead: working towards effective clinical translation of myocardial gene therapies. *Ther. Deliv*. 5(1):39–51, 2014.
[17]Kullberg, M., R. McCarthy, and T. J. Anchordoquy. Systemic tumor-specific gene delivery. *J. Control Release*. 172(3):730–736, 2013.
[18]Lentacker, I., N. Wang, R. E. Vandenbroucke, J. Demeester, S. C. De Smedt, and N. N. Sanders. Ultrasound exposure of lipoplex loaded microbubbles facilitates direct cytoplasmic entry of the lipoplexes. *Mol. Pharm*. 6(2):457–467, 2009.
[19]Mehier-Humbert, S., and R. H. Guy. Physical methods for gene transfer: improving the kinetics of gene delivery into cells. *Adv. Drug. Deliv. Rev*. 57(5):733–753, 2005.
[20]Murciano, J. C., S. Muro, L. Koniaris, M. Christofidou-Solomidou, D. W. Harshaw, S. M. Albelda, D. N. Granger, D. B. Cines, and V. R. Muzykantov. ICAM-directed vascular immunotargeting of antithrombotic agents to the endothelial luminal surface. *Blood* 101(10):3977–3984, 2003.
[21]Nam, J. P., and J. W. Nah. Target gene delivery from targeting ligand conjugated chitosan-PEI copolymer for cancer therapy. *Carbohydr. Polym*. 135:153–161, 2016.
[22]Nia, A. H., A. Amini, S. Taghavi, H. Eshghi, K. Abnous, and M. Ramezani. A facile Friedel-Crafts acylation for the synthesis of polyethylenimine-grafted multi-walled carbon nanotubes as efficient gene delivery vectors. *Int. J. Phar*. 502(1–2):125–137, 2016.
[23]Panje, C. M., D. S. Wang, and J. K. Willmann. Ultrasound and microbubble-mediated gene delivery in cancer: progress and perspectives. *Invest. Radiol*. 48(11):755–769, 2013.
[24]Prasad, G., H. Wang, D. L. Hill, and R. Zhang. Recent advances in experimental molecular therapeutics for malignant gliomas. *Curr. Med. Chem. Anticancer Agents*. 4(4):347–361, 2004.
[25]Qian, L., B. Thapa, J. Hong, Y. Zhang, M. Zhu, M. Chu, J. Yao, and D. Xu. The present and future role of ultrasound targeted microbubble destruction in preclinical studies of cardiac gene therapy. *J. Thorac. Dis*. 10(2):1099–1111, 2018.
[26]Qiu, Y., Y. Luo, Y. Zhang, W. Cui, D. Zhang, J. Wu, J. Zhang, and J. Tu. The correlation between acoustic cavitation and sonoporation involved in ultrasound-mediated DNA transfection with polyethylenimine (PEI) in vitro. *J. Control Release* 145(1):40–48, 2010.
[27]Roger, V. L., A. S. Go, D. M. Lloyd-Jones, E. J. Benjamin, J. D. Berry, W. B. Borden, D. M. Bravata, S. Dai, E. S. Ford, C. S. Fox, H. J. Fullerton, C. Gillespie, S. M. Hailpern, J. A. Heit, V. J. Howard, B. M. Kissela, S. J. Kittner, D. T. Lackland, J. H. Lichtman, L. D. Lisabeth, D. M. Makuc, G. M. Marcus, A. Marelli, D. B. Matchar, C. S. Moy, D. Mozaffarian, M. E. Mussolino, G. Nichol, N. P. Paynter, E. Z. Soliman, P. D. Sorlie, N. Sotoodehnia, T. N. Turan, S. S. Virani, N. D. Wong, D. Woo, M. B. Turner, and American Heart Association Statistics, C.; Stroke Statistics, S. Executive summary: heart disease and stroke statistics–2012 update: a report from the American Heart Association. *Circulation* 125(1):188–197, 2012.
[28]Stride, E. Physical principles of microbubbles for ultrasound imaging and therapy. *Front. Neurol. Neurosci*. 36:11–22, 2015.
[29]Sun, L., C. W. Huang, J. Wu, K. J. Chen, S. H. Li, R. D. Weisel, H. Rakowski, H. W. Sung, and R. K. Li. The use of cationic microbubbles to improve ultrasound-targeted gene delivery to the ischemic myocardium. *Biomaterials* 34(8):2107–2116, 2013.
[30]Sun, Y. X., J. Y. Zhu, W. X. Qiu, Q. Lei, S. Chen, and X. Z. Zhang. Versatile supermolecular inclusion complex based on host-guest interaction for targeted gene delivery. *ACS Appl. Mater. Interfaces*. 9(49):42622–42632, 2017.
[31]Unger, E., T. Porter, J. Lindner, and P. Grayburn. Cardiovascular drug delivery with ultrasound and microbubbles. *Adv. Drug Deliv. Rev*. 72:110–126, 2014.
[32]Wang, D. S., C. Panje, M. A. Pysz, R. Paulmurugan, J. Rosenberg, S. S. Gambhir, M. Schneider, and J. K. Willmann. Cationic versus neutral microbubbles for ultra-

sound-mediated gene delivery in cancer. *Radiology* 264(3):721–732, 2012.
[33]Yan, P., K. J. Chen, J. Wu, L. Sun, H. W. Sung, R. D. Weisel, J. Xie, and R. K. Li. The use of MMP2 antibody-conjugated cationic microbubble to target the ischemic myocardium, enhance Timp3 gene transfection and improve cardiac function. *Biomaterials*. 35(3):1063–1073, 2014.
[34]Yan, Y., Y. Liao, L. Yang, J. Wu, J. Du, W. Xuan, L. Ji, Q. Huang, Y. Liu, and J. Bin. Late-phase detection of recent myocardial ischaemia using ultrasound molecular imaging targeted to intercellular adhesion molecule-1. *Cardiovasc. Res*. 89(1):175–183, 2011.
[35]Yang, J., H. Liu, and X. Zhang. Design, preparation and application of nucleic acid delivery carriers. *Biotechnol. Adv*. 32(4):804–817, 2014.
[36]Yang, H., X. Xiong, L. Zhang, C. Wu, and Y. Liu. Adhesion of bio-functionalized ultrasound microbubbles to endothelial cells by targeting to vascular cell adhesion molecule-1 under shear flow. *Int. J. Nanomed*. 6:2043–2051, 2011.
[37]Yu, Z. Q., J. J. Yan, Y. Z. You, and Q. H. Zhou. Bioreducible and acid-labile poly(amido amine)s for efficient gene delivery. *Int. J. Nanomed*. 7:5819–5832, 2012.
[38]Zafir-Lavie, I., S. Sherbo, H. Goltsman, F. Badinter, E. Yeini, P. Ofek, R. Miari, O. Tal, A. Liran, T. Shatil, S. Krispel, N. Shapir, G. A. Neil, I. Benhar, A. Panet, and R. Satchi-Fainaro. Successful intracranial delivery of trastuzumab by gene-therapy for treatment of HER2-positive breast cancer brain metastases. *J. Control Release*. 291:80–89, 2018.
[39]Zhu, L., and R. I. Mahato. Lipid and polymeric carrier-mediated nucleic acid delivery. *Expert. Opin. Drug Deliv*. 7(10):1209–1226, 2010.